Bulletin of Electrical Engineering and Informatics
Vol. 14, No. 1, February 2025, pp. 132~142
ISSN: 2302-9285, DOI: 10.11591/eei.v14i1.8618

Variable loaded brushless DC motor with six step commutation PID-based speed controller optimized by PSO algorithm

Fitriaty Pangerang[1,3], Faizal Arya Samman[1], Zahir Zainuddin[2], Rhiza S. Sadjad[1]
[1]Department of Electrical Engineering, Hasanuddin University, Gowa, South Sulawesi, Indonesia
[2]Department of Informatics, Hasanuddin University, Gowa, South Sulawesi, Indonesia
[3]Department of Electrical Engineering, Politeknik Negeri Ujung Pandang, Makassar, South Sulawesi, Indonesia

Article Info

Article history:

Received Apr 24, 2024
Revised Aug 14, 2024
Accepted Aug 25, 2024

Keywords:

Brushless DC motors
Particle swarm optimization
Proportional integral derivative
Six commutations
Speed controller

ABSTRACT

This research presents a method for regulating varying voltage as a DC source in a six-step commutation brushless DC (BLDC) motor drive through control proportional integral derivative (PID) as a simple strategy for controlling the speed of BLDC motors. Strengthening the control gain uses the particle swarm optimization (PSO) algorithm by minimizing the root mean square error (RMSE) and overshoot as fitness control characteristics. The performance of the motor with the proposed controller is analyzed and compared with an experimentally-simulated-tuned PID, hybrid gray wolf optimization–proportional integral (GWO-PI), and hybrid horse herd PSO-PID (HHH PSO-PID) under changing load and speed conditions. Simulation using compose-psim altair software. Control system response parameters such as RMSE, overshoot, electromagnetic torque ripple, and phase current ripple are measured and compared with the above controllers. The results show that the proposed controller is superior to a wide range of predefined system responses.

Corresponding Author:

Faizal Arya Samman
Department of Electrical Engineering, Hasanuddin University
Jl. Poros Malino, km 6, Bontomarannu, Gowa, Makassar, 92171 South Sulawesi, Indonesia
Email: faizalas@unhas.ac.id

1. INTRODUCTION

Brushless DC (BLDC) motors are an essential element for most real-life applications. It has been widely used in many industrial, household, commercial, and automotive applications over the past few years due to its advantages such as control flexibility, high torque capability, silent operation, more efficiency, smaller size, and volume compared to conventional motors [1]–[3]. In general, a BLDC consists of a rotor, which is made of permanent magnets, and a stator, which is made of a 3-phase coil. Even though it is a 3-phase AC synchronous electric motor, this motor is still called BLDC because in its implementation it uses a DC source as the main energy source which is then converted into AC voltage using a 3-phase inverter. The purpose of providing 3-phase AC voltage to the stator is to create a rotating stator magnetic field to attract the rotor magnet. The commutation process depends on the position of the rotor, where the rotational speed is regulated by the applied voltage. Therefore, in controlling it is necessary to have the right commutation change timing so that the motor speed is constant [4]–[6].

The six-step commutation method is a method that is often used to determine commutation change timing because it is easy to implement and has a simple algorithm but has a higher rms current which causes torque ripples and overshoot, especially in a wide speed range [7]–[9]. In the six-step method, the motor speed is regulated by reducing or increasing the voltage at the input and it becomes inefficient, because the greater the load will affect the motor speed, it is necessary to add voltage so that the speed increases because

if not, the voltage required by the motor will not be achieved perfectly. This condition causes the speed control of the BLDC motor to obtain the desired acceleration to become more difficult, especially under load conditions.

Various control methods have been implemented such as controlling the voltage source inverter which has a current controlled control system, speed is controlled by keeping the voltage at the system terminal constant by controlling the inverter output current [10]–[12]. The disadvantage is that the number of semiconductor components is greater with a more complicated circuit structure. The hysteresis current control method uses a reference current and an actual current. The actual current can continuously follow the motor reference current within a hysteresis band, which is the upper and lower limits of the allowable error size [13]–[15], but the switching frequency sometimes changes. Voltage mode control represents the most basic method, where only the output voltage is returned via a feedback loop [16]–[18], the advantage is its simplicity, but it creates harmonic currents and voltages on both sides of the DC and AC voltages which give rise to large current and torque ripples.

The ability of the control method to control motor speed is also greatly determined by the choice of controller. The fuzzy logic controller on [19]–[21] can control BLDC motors and can solve problems of uncertainty and sudden disturbances but the design depends on experience which is sometimes not available for some systems. Neural network research [22]–[24] can handle uncertainty and nonlinear parameters but requires a larger storage capacity to store neuron weights and parameters. Proportional integral derivative (PID) controller has a simple structure and is easy to implement [25], [26]. However, it can only be used for linear systems because PID control optimization is constrained by drive systems that work under fluctuating operating conditions, so the optimal value of PID gain is difficult to determine.

The accuracy of determining the optimal value of control gain depends on the selection of appropriate algorithms, the concept is to choose an optimization technique with less computational effort and a higher level of convergence performance. Gajić *et al.* [27], introduced the particle swarm optimization (PSO) evolutionary algorithm as an optimization technique, the main idea and structure of this algorithm are inspired by evolutionary computing. This algorithm is considered one of the leading swarm intelligence algorithms with its ease of implementation, fast discovery of various high-quality solutions, simple operation, and stable convergence characteristics [28]–[30].

This research introduces an approach to a BLDC motor speed control method in voltage mode control with a voltage-controlled DC bus voltage control mechanism. The voltage supply to the inverter uses a controlled source voltage, based on a comparison of the reference speed and the actual motor speed through a feedback loop. Simplicity is maintained by controlling the DC bus voltage with closed-loop negative feedback that keeps the loop gain constant over varying input voltages. PID control is used so that the simplicity of the structure is maintained. PSO algorithm for strengthening control gain with control characteristics of minimum root mean square error (RMSE) and minimum overshoot. The control target is that the motor speed remains stable with minimum torque ripple, current ripple, and overshoot even under load conditions and speed changes.

The research we present contributes to introducing a simple and easy control method and little computation in the algorithm so that it can reduce electrical power consumption in its application, but remains efficient, especially in a wide speed range. To present ideas clearly, this research is structured as follows. Section 2 discusses mathematical modeling and the concept of a 3 phase six-step commutation inverter, and section 3 discusses the proposed control method in the form of a system diagram and control structure used. Section 4 analysis of simulation results of the proposed control method and comparison with experimentally-simulated-tuned PID, hybrid gray wolf optimization–proportional integral (GWO-PI) [31], and hybrid horse herd PSO [32]. Simulation results are presented under varying loading and speed conditions. Section 5 is conclusion.

2. MATHEMATICAL MODELING AND 3-PHASE SIX-STEP COMMUTATION INVERTER SYSTEM

2.1. Brushless DC mathematical modeling

Mathematical modeling is used to formally represent the dynamics and behavior of BLDC motors which helps in understanding how BLDC motors respond to changes in speed and control input. The next stage is that this mathematical model is integrated into the control algorithm design. The mathematical model of a three-phase BLDC motor is illustrated.

$$Va = R.i_a + (L - M).\frac{di_a}{dt} + E_a \quad (1)$$

$$Vb = R.i_b + (L - M).\frac{di_b}{dt} + E_b \quad (2)$$

$$Vc = R.i_c + (L - M).\frac{di_c}{dt} + E_c \quad (3)$$

where Va, Vb, and Vc are the phase voltages, i_a, i_b, and i_c are the phase currents, R, L, and M are the stator phase resistance, self-inductance, and mutual inductance, and E_a, E_b, and E_c are the back emf of phase A, B, and C, respectively. The back emf voltages are a function of the rotor mechanical speed ω_m and the rotor electrical angle θ_r, that is:

$$E_a = k_{e-a}.\omega_m \quad (4)$$

$$E_b = k_{e-b}.\omega_m \quad (5)$$

$$E_c = k_{e-c}.\omega_m \quad (6)$$

The coefficients k_{e-a}, k_{e-b}, and k_{e-c} are dependent on the rotor angle θ_r.

$$K_{pk} = \frac{V_{pk/K_{rpm}}}{2}.\frac{60}{1000.2\pi} \quad (7)$$

where K_{pk} the trapezoidal peak value expressed in V/(rad./sec). The developed torque of the machine is (8):

$$T_{em} = \frac{E_a.i_a + E_b.I_b + E_c.I_c}{\omega_m} \quad (8)$$

The mechanical are (9) and (10):

$$J.\frac{d\omega_m}{dt} = T_{em} - B.\omega_m - T_{Load} \quad (9)$$

$$\frac{d\theta_r}{dt} = \frac{P}{2}\omega_m \quad (10)$$

where ω_m is the mechanical speed in rad./sec, B is the friction coefficient, T_{Load} is the load torque, and P is the number of poles. The coefficient B is calculated from the moment of inertia J and the shaft time constant τ_{shaft} as (11):

$$B = \frac{J}{\tau_{shaft}} \quad (11)$$

The shaft time constant τ_{shaft}, therefore, reflects the effect of the friction and windage of the machine. Table 1 shows BLDC motor parameters.

Table 1. BLDC motor parameters

Parameter	Values
Stator resistance (R)	11.9 ohms
Stator self-inductance (L)	0.002080 H
Stator mutual inductance (M)	-0.00069 H
Peak ine-to-line back emf constant	32.3 V/rpm
Rms line-to-line back emf constant	22.9 Vrms/crpm
Pole	4
Moment of inertia	7.10-6 kgm^2
Shaft time is constant	0.006 seconds
Conduction pulse width	120 electrical deg
Slave flags	1
Torque flag	1

2.2. Inverter 3 phase six-step commutation brushless DC motor

The electronic commutation method is a six-step commutation, namely changing the polarity of the coil in six stages to produce one full rotation, shown in Figure 1. Commutation occurs every 60 electrical degrees, to complete one electrical cycle (360 electrical degrees) consisting of six different steps. In this system, the magnetic field from the coil will be read by three hall effect sensors (H1, H2, and H3) which are installed on the stator at 120^o intervals. Every 60^o rotations, one hall sensor changes its state, which then

provides a trapezoidal signal to the changeover control process to determine the rotor position which is divided into six different parts, as a motor drive switching configuration using a mosfet. The positive part is for switches S1, S3, and S5 and the negative part is for switches S2, S4, and S6, set to on and off conditions. The six-step switching configuration carried out continuously will produce a rotation ratio of 360°.

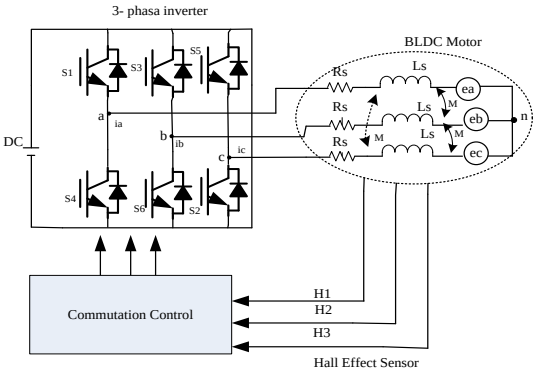

Figure 1. 3-phase inverter

3. PROPOSED METHOD

3.1. System diagram

The proposed control scheme diagram is shown in Figure 2. The system consists of a DC voltage source, a six-step commutation inverter circuit, and a PID controller. The source voltage will be controlled by a DC-DC converter and produce a controlled output voltage activating a six-step commutation inverter circuit which produces 3 three-phase currents. The signal given to the converter will determine the value of the output voltage. This signal is a function of the amplification factor (duty cycle) on the switch, namely the comparison of time between the on condition of the switch to one switching period. By setting the work factor, the output voltage can be adjusted. The hall effect sensor will detect the magnetic field from the coil passing through it. The hall effect sensor then provides data signals to the commutation control, regulating the commutation of the BLDC motor. The output voltage produced by the controlled source voltage is shown in (12) to (14):

$$V_{out} = k.V_{in} \tag{12}$$

$$V_{out} = \frac{T_{on}}{T_{on} + T_{off}} V_{in} \tag{13}$$

$$V_{out} = D.V_{in} \tag{14}$$

where, V_{out} is controlled output voltage, V_{in} is source voltage, k is gain factor, T_{on} is on period, T_{off} is off period, and D is duty cycle.

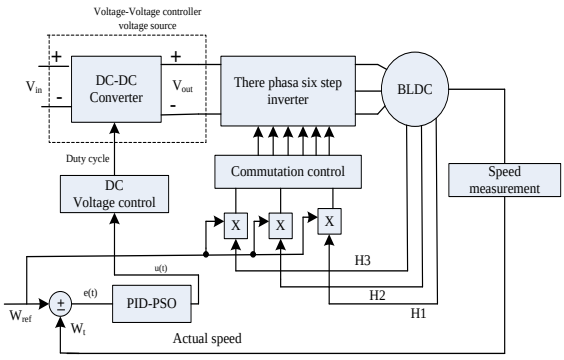

Figure 2. Diagram of the proposed BLDC motor speed control system

3.2. Proportional integral derivative control algorithm structure

PID control gain consists of proportional (Kp), integral (Ki), and derivative (Kd). The three control gains are added to produce the control signal u(t). The control is shown (15) and (16):

$$u(\mathrm{t}) = \mathrm{K_p e(t)} + \mathrm{K_i} \int \mathrm{e(t)dt} + \mathrm{K_d} \frac{\mathrm{de}}{\mathrm{dt}} \quad (15)$$

$$u(t) = K_p \left[e(t) + \frac{1}{T_i} \int_0^1 e * dt + T_d \frac{de(t)}{dt} \right] \quad (16)$$

The error signal is formulated as (17):

$$e(t) = W_{ref} - W_t \quad (17)$$

To implement a PID controller using a digital computer, the continuous (15) is converted to a difference equation using the direct discretization equation method. The integral part is defined as the total area formed by the error from the beginning to the last error.

$$\int_0^t e(t)dt = e_{int-1} + \left(\frac{(e_t + e_{t-1})T}{2} \right) \quad (18)$$

The derivative part is defined as the change in error over time as shown by (19):

$$\frac{de(t)}{dt} = \frac{e(nT) - e(nT-T)}{T} \quad (19)$$

Substituting (18) and (19) above into (16) then we get (20):

$$u(nT) = K_p \left(e(nT) + \frac{1}{T_i} \left(e_{int-1} + \left(\frac{(e_t + e_{t-1})T}{2} \right) \right) + T_d \frac{e_n - e_{n-1}}{T} \right) \quad (20)$$

In (20) to calculate the controller output, it requires an initial error value ($u_n t$= 0) until (last error calculation time). The integral error calculation for realization in embedded systems is shown in (21):

$$e_{int} = e_{int-1} + e_{int\_update} \quad (21)$$

where $e(t)$ is current error, e_{int-1} is error area before the latest error calculation e(t), e_{t1} is previous error, e_{int_update} is area formed by the current error and the previous error, e_{int} is integral error, T is time sampling, W_{ref} is reference speed, and W_t is actual speed.

3.3. Proportional integral derivative control gain

PID control gain using algorithm PSO. PSO is a technique based on the natural properties of certain groups of animals, such as ants, bees, termites, and birds [33]. In PSO there are three important components, including particles, cognitive components, and social components, as well as particle speed. Each particle adjusts to the best position of the particle (local best) and adjusts the position of the best particle from the best value of the entire flock (global best) while traversing the search space at each iteration. The best particle position solution uses a fitness function [30].

Position (L) is a set of position vectors in a swarm, the position vector for the -1, particle is defined as Li=$[l_{ik}]$=$\left[l_{i1}, l_{i2} \ldots l_n\right]$ where i is the number of particles in a swarm (sw_size), k={1,2,3,…n}, and n is the number of locations. Velocity vectors in a swarm are denoted as $[v_{ik}] = [v_{i1}, v_{i2} \ldots \ldots v_{in}]$. Personal best, denoted P={Pi}, is the set of best position vectors for the ith particle in a particular iteration, and Pi=[P_{ik}]=[p_{i1}, p_{i2}, …, p_{in}], with a position value of Pbest to -*i* is related to -*k* the dimension. The personal best value of each particle at each iteration *t* is updated if a better fitness value is obtained. The personal best fitness value at iteration (*t)* is the smallest fitness value for each particle for the initial iteration (iteration -1) to iteration -*t*. One personal best with the best fitness value for the entire swarm at a particular iteration is called the global best and denoted G=[g_1, g_2, …, g_n].

The speed is updated at each iteration to move the original position to a better position. Let is the component of the velocity vector to *i* (v_i) on the th iteration -*t*, then update the velocity vector components to -*i* on the th iteration *t+1*. In (22) is used:

$$v_{ik}^{(t+1)} = w.v_{ik}^{(t)} + c_1 r_1\left(p_{ik}^{(t)} - i_{ik}^{(t)}\right) + c_2 r_2\left(g_k^{(t)} - i_{ik}^{(t)}\right) \quad (22)$$

where: w is the inertial weight that is generated randomly in the interval [0,1], c_1 and c_2 are social and cognitive parameters and t is the many iterations, r_1 and $r_2$random numbers at intervals [0,1]. After getting the new velocity vector components, the position vector components are updated using (23):

$$l_{ik}^{(t+1)} = l_{ik}^{(t)} + v_{ik}^{(t+1)} \quad (23)$$

where, $l_{ik}^{(t+1)}$ is the position vector of the ith particle.

The steps of the proposed algorithm are as follows:

a. Initialize PSO parameters. PSO parameters are shown in Table 2.
b. Evaluate the fitness value. The fitness value is the reliability of particles to survive in a population (swarm). The smaller the fitness value is directly proportional the more reliable the particle is to survive in a swarm. The fitness values used in this research use (24) and (25):

Function $Fitness = min\ [(RMSE\ )] + min\ [(Mp)]$ (24)

Function $Fitness = \min\left[\left(\sum_{i=1}^{N}\left(\frac{(Vt-Vi)^2}{n}\right)\right)\right] + \min[(\max(Vt) - (Vref)]$ (25)

where, n is the total number of predicted data, Vt is actual speed, Vi is speed from the predicted results, $Vref$ is reference speed value, $min\ [(Mp)]$ is minimum overshoot value, and $min\ [(RMSE)]$ is minimum RMSE value.

c. Update the particle velocity using (22).
d. Update the particle position using (23).
e. The main loop and fitness function start doing their calculations to update the particle positions at each iteration. If the new amount is superior to the previous Pbest then the new amount is adjusted to Pbest compatible, and the number of gbest is also updated as a better Pbest.
f. The process of searching for the best particle position continues until the number of iterations is reached and the PID gain value is obtained at the minimum RMSE and overshoot conditions from all existing iterations.

Table 2. Parameters of the PSO algorithm

Parameters	Value
Lower-bound (lower limit for Kp, Ki, Kd)	[0.00005, 0.0005, 0.00005]
Upper-bound (upper limit for Kp, Ki, Kd)	[0.00015, 0.0015, 0.00015]
maximum iterations	100
Number of populations	30
Inertia coefficient (w)	1
Damping factor (wdamp)	0.8
Personal acceleration coefficient (c_1)	9
Social acceleration coefficient (c_2)	9

4. RESULTS AND DISCUSSION

Testing and simulation of control designs are evaluated in the psim altair simulator platform. In this simulation, the BLDC motor is operated for 2 seconds and given a load of 1.8 Nm, with a speed change from 1,000 RPM to 3,000 RPM, from 3,000 RPM to 1,000 RPM. The purpose of the simulation is to determine the ability of the proposed control to respond to reference speed, electromagnetic torque, and 3-phase current when speed changes occur with loading. The simulation results are compared with the control method in Table 3.

Table 3. Control gain parameters

Control method	Kp	Ki	Kd
Experimentally-simulated-tuned PID	0.0001	0.001	0.0001
PSO-PID (proposed)	0.000139	0.00182	0.0000899
HHH PSO-PID [32]	0.35	1.25	0.05
GWO-PI [31]	0.01	0.01	-

4.1. Motor speed response

The purpose of the test is to determine the response of the motor's actual speed to the reference speed. The signal plot in Figure 3 shows that there is a speed spike in all control methods when the motor starts to operate. Unless the trial and error PID method is no longer able to respond to the initial speed. When a change in speed occurs, only the proposed control can respond to the speed without oscillations, while the other controllers experience oscillations. The control signal response was also analyzed in terms of RMSE and overshoot percentage criteria, the results are presented in Table 4. The proposed controller has a smaller RMSE and overshoot error percentage, these results show that the performance of the control system in responding to speed is superior to other compared control methods.

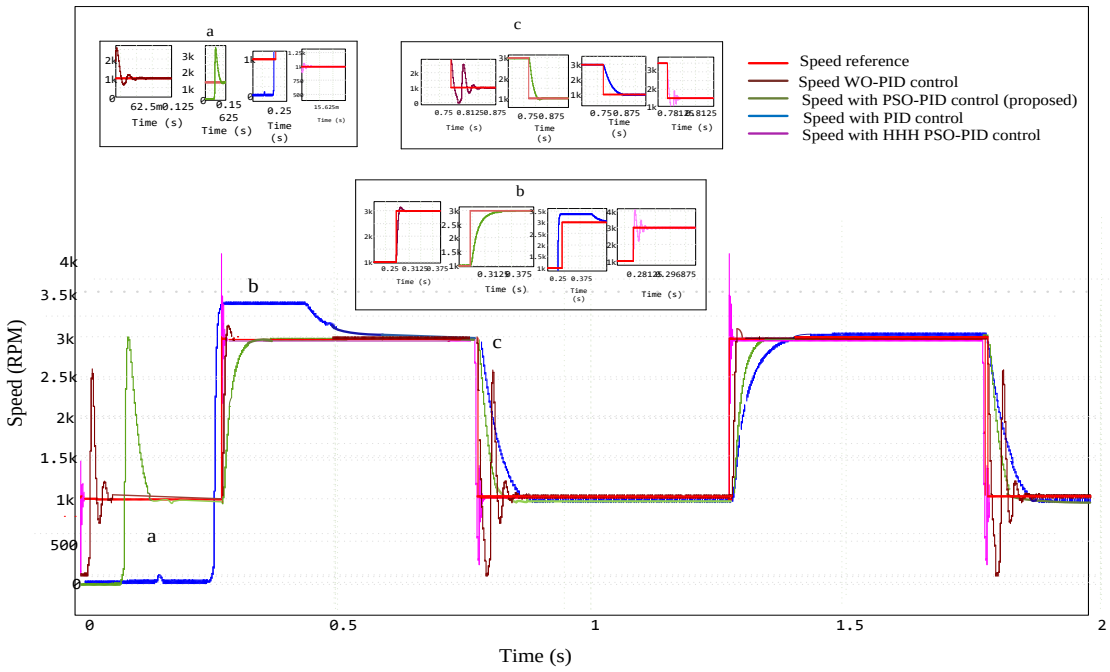

Figure 3. BLDC motor speed response

Table 4. Control system performance in response to BLDC motor speed

Control method	RMSE	Overshoot (%)
Experimentally-simulated-tuned PID	601.31056	237,411
PSO-PID (proposed)	495.300627	200.48
HHH PSO-PID	1963.74238	214.37
GWO-PI	541.105396	237.41

4.2. Electromagnetic torque response

This test aims to see the response of electromagnetic torque to changes in motor speed when loading occurs. The signal response is shown in Figure 4. In Figures 4(a) and (b), the signal response shows a spike in torque with large oscillations when there is a change in speed, this condition lasts as long as the motor is operating. Meanwhile Figure 4(c), it shows the occurrence of a torque spike with a long interval, at the initial speed. In the proposed control method, Figure 4(d), the signal response shows a torque spike, but in a short time interval only at the initial speed, and the signal response returns to stability. Compared with other methods, it shows that the electromagnetic torque response of the proposed control method can adjust its torque to changes in speed compared to other methods.

In this test, torque ripple was also measured, as shown in Table 5. The results show that the proposed control method has a smaller percentage of electromagnetic torque ripple compared to other control methods. Formula for torque ripple [34], shown in (26):

$$Torque\ ripple = \frac{(T_{max} - T_{min})}{T_{Avg}}\ x\ 100\ \% \quad (26)$$

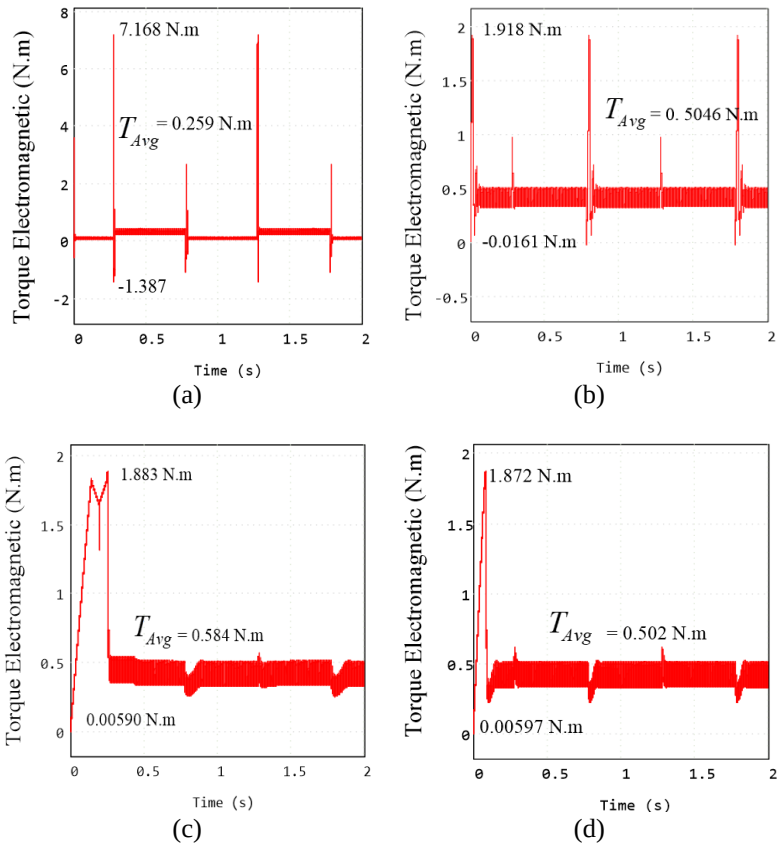

Figure 4. Electromagnetic torque: (a) HHH PSO-PID, (b) GWO-PI, (c) experimentally-simulated-tuned PID, and (d) proposed method

Table 5. Torque ripple percentage

Control method	Tmax (Nm)	Tmin (Nm)	Average torque (Nm)	Ripple torque (%)
Experimentally-simulated-tuned PID	1,883	0.00590	0.584	321.4212
PSO-PID (proposed)	1,872	0.00597	0.582	320.6237
HHH PSO-PID	7,168	-1,387	0.259	3291.21
GWO-PI	1.91	-0.0161	0.5046	383,348

4.3. 3-phase current response

This test aims to determine the phase current response in the BLDC motor stator when changes in speed and loading occur. The signal response is shown in Figure 5. In this test, the total harmonics distortion is measured to determine the magnitude of the ripples generated by each phase, the THD formula [35] shown in (27):

$$THD = \frac{\sqrt{\sum_{h>1}^{hmax} M_h^2}}{M_1} \quad (27)$$

where, THD is total harmonic distortion, M_h is rms value of harmonic current to-h, and M_1 is rms value of the current at the basic frequency.

In Figure 5(a), current fluctuations occur in each phase, reaching 25 amperes and occur with changes in motor speed, likewise in Figure 5(b), current fluctuations occur up to 6.3 amperes. In Figure 5(c), a current surge of 6.2 amperes with a long duration occurs at the initial speed. In the proposed control method, Figure 5(d) a current surge also occurs at 6 amperes and lasts briefly at the initial speed. The phase current spike that occurs is smaller compared to other methods, this condition shows that the electric current consumption in the proposed control method is relatively small. The THD is shown in Table 6. A lower THD is produced by the proposed controller, indicating that the resulting current ripple is less compared to other methods.

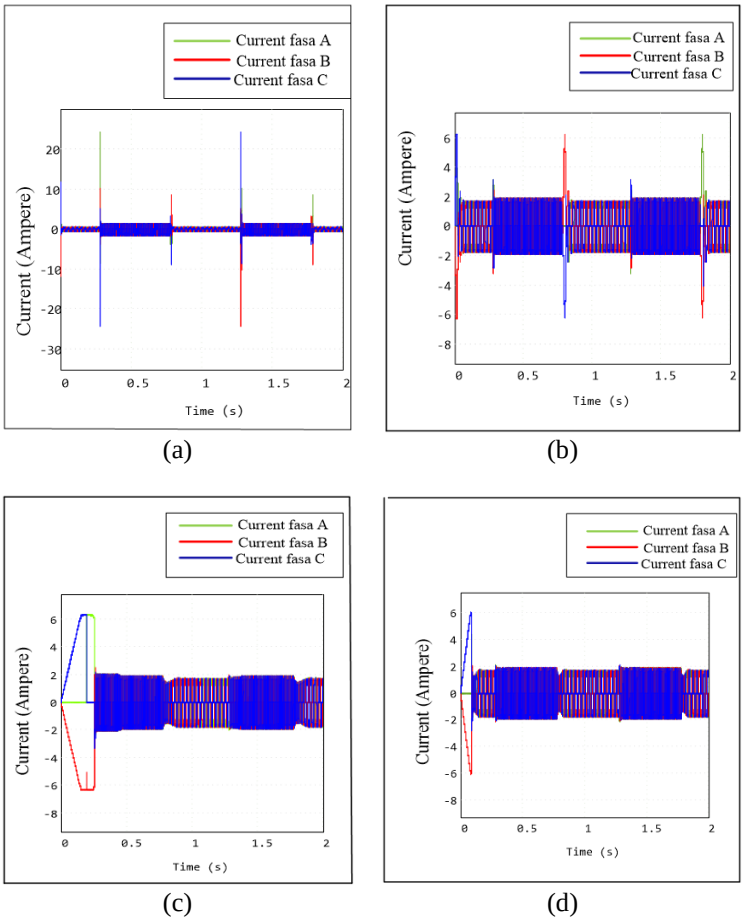

Figure 5. BLDC motor phase current response: (a) HHH PSO-PID, (b) GWO-PI, (c) experimentally-simulated-tuned PID, and (d) proposed method

Table 6. THD of 3-phase current

Method	THD 3 phase current (amperes)		
	Phase current (Ia)	Phase current (Ib)	Phase current (Ic)
Experimentally-simulated-tuned PID	1,517	1,062	121,570
PID–PSO (proposed)	0.775	1,470	0.867
HHH PSO-PID	20,636	1,343	1,206
GWO-PI	2,210	96,988	9,311

5. CONCLUSION

In this study, simple but effective speed control is achieved using the proposed PSO-based PID controller for BLDC motors. The proposed controller is compared with other controllers under varying loading and speed conditions. Control system performance such as RMSE, overshoot, and the influence of control on electromagnetic torque ripple, 3-phase current ripple, and phase current THD have been measured, analyzed, and compared. The results show that the PID-PSO controller outperforms other controllers in responding to reference speed, reducing current ripple and electromagnetic torque ripple, with smaller RMSE, current ripple, and electromagnetic torque ripple values. The proposed method can improve the speed response performance of BLDC motors, especially over a wide speed range. However, further research is still needed regarding reducing current surges, especially at initial speeds.

ACKNOWLEDGEMENTS

The authors gratefully acknowledge the ministry of education, culture, research, and technology of the Republic of Indonesia for financial support of the research under the scheme of the doctoral dissertation research program in the year of 2023-2024, with grant contract number 02381/UN4.22/PT.01.03/2023.

REFERENCES

[1] K. Sayed, H. H. El-Zohri, A. Ahmed, and M. Khamies, "Application of Tilt Integral Derivative for Efficient Speed Control and Operation of BLDC Motor Drive for Electric Vehicles," *Fractal and Fractional*, vol. 8, no. 1, 2024, doi: 10.3390/fractalfract8010061.

[2] D. Mohanraj *et al.*, "A Review of BLDC Motor: State of Art, Advanced Control Techniques, and Applications," *IEEE Access*, vol. 10, pp. 54833–54869, 2022, doi: 10.1109/ACCESS.2022.3175011.

[3] I. Anshory, "Performance Analysis Stability Of Speed Control Of BLDC Motor Using PID-BAT Algorithm In Electric Vehicle," *JEEE-U (Journal of Electrical and Electronic Engineering-UMSIDA)*, vol. 1, no. 1, pp. 22–28, 2017, doi: 10.21070/jeee-u.v1i1.757.

[4] M. F. Sachruddin, F. A. Samman, and R. S. Sadjad, "BLDC Motor Control using a Complex Programmable Logic Device with Hall-Sensors," *ICSGTEIS 2021-2021 International Conference on Smart-Green Technology in Electrical and Information Systems: Advancing Smart and Green Technologies Toward Society 5.0, Proceedings*, 2021, pp. 7–11, doi: 10.1109/ICSGTEIS53426.2021.9650433.

[5] Q. Zhang and M. Feng, "Combined commutation optimisation strategy for brushless DC motors with misaligned hall sensors," *IET Electric Power Applications*, vol. 12, no. 3, pp. 301–307, 2018, doi: 10.1049/iet-epa.2017.0276.

[6] X. Cao, J. Liu, D. Wang, C. Wu, and J. Tian, "Design of a Two-phase Brushless DC Motor Control System," *Journal of Physics: Conference Series*, vol. 2417, no. 1, pp. 0–7, 2022, doi: 10.1088/1742-6596/2417/1/012028.

[7] H. Y. O. Yang and R. D. Lorenz, "Torque ripple minimization in six-step PMSM drives via variable and fast DC Bus Dynamics," *IEEE Transactions on Industry Applications*, vol. 55, no. 4, pp. 3791–3802, 2019, doi: 10.1109/TIA.2019.2910450.

[8] A. El Ghaly, "Simplified Control for Torque and Speed Ripple Mitigation in Brushless DC Motors," *International Journal of Smart grid*, vol. 8, no. 1, 2024, doi: 10.20508/ijsmartgrid.v8i1.321.g325.

[9] V. Krishnakumar, N. Madhanakkumar, P. Pugazhendiran, C. Bharathiraja, and V. Sriramkumar, "Torque ripple minimization of PMBLDC motor using simple boost inverter," *International Journal of Power Electronics and Drive Systems*, vol. 10, no. 4, pp. 1714–1723, 2019, doi: 10.11591/ijpeds.v10.i4.pp1714-1723.

[10] N. Hidayat, F. A. Samman, and R. S. Sadjad, "FPGA Based Controller of BLDC Motor Using Trapezoid Control," *ICITEE 2022 - Proceedings of the 14th International Conference on Information Technology and Electrical Engineering*, 2022, pp. 58–63, 2022, doi: 10.1109/ICITEE56407.2022.9954075.

[11] S. D. Kim, T. V. Tran, S. J. Yoon, and K. H. Kim, "Current Controller Design of Grid-Connected Inverter with Incomplete Observation Considering L-/LC-Type Grid Impedance," *Energies*, vol. 17, no. 8, 2024, doi: 10.3390/en17081855.

[12] S. A. Azmi, G. P. Adam, S. R. A. R. Rahim, and B. W. Williams, "Current control of grid connected three phase current source inverter based on medium power renewable energy system," *International Journal of Advanced Technology and Engineering Exploration*, vol. 8, no. 74, pp. 34–44, 2021, doi: 10.19101/IJATEE.2020.S2762172.

[13] J. K. Singh and R. K. Behera, "Hysteresis Current Controllers for Grid Connected Inverter: Review and Experimental Implementation, " *2018 IEEE International Conference on Power Electronics, Drives and Energy Systems (PEDES)*, Chennai, India, 2018, pp. 1-6, doi: 10.1109/PEDES.2018.8707755.

[14] Zulkhairi, M. Facta, T. Andromeda, Hermawan, and I. Setiawan, "Single Phase AC Current Controller by Using Hysteresis Method," *E3S Web of Conferences*, vol. 125, pp. 2–6, 2019, doi: 10.1051/e3sconf/201912514004.

[15] A. M. S. Yunus, S. Swasti, and Purwito, "Overview of Hysteresis Current Controller Application in Renewable Energy Based Power Systems," *IOP Conference Series: Materials Science and Engineering*, vol. 536, no. 1, 2019, doi: 10.1088/1757-899X/536/1/012048.

[16] B. Johnson, S. Salapaka, B. Lundstrom, and M. Salapaka, "Optimal Structures for Voltage Controllers in Inverters Preprint Optimal Structures for Voltage Controllers in Inverters," *Presented at the IEEE International Symposium on Mathematical Theory of Networks and Systems Minneapolis*, Minnesota, 2016, pp. 1–6.

[17] Y. Asadi, M. Eskandari, M. Mansouri, A. V. Savkin, and E. Pathan, "Frequency and Voltage Control Techniques through Inverter-Interfaced Distributed Energy Resources in Microgrids: A Review," *Energies*, vol. 15, no. 22, 2022, doi: 10.3390/en15228580.

[18] H. Tang *et al.*, "Robust Voltage Control of a Single-Phase UPS Inverter Utilizing LMI-Based Optimization with All-Pass Filter Under System Uncertainty," *International Journal of Robotics and Control Systems*, vol. 4, no. 2, pp. 910–928, 2024, doi: 10.31763/ijrcs.v4i2.1452.

[19] C A. Kumar, B. R. Harijan, M K. Kumar, and M. Bharathi, "BLDC Motor Speed Control using Fuzzy Logic PID Controller and Comparing It With PI Controller," *International Journal of Engineering and Advanced Technology*, vol. 9, no. 2, pp. 4917–4922, 2019, doi: 10.35940/ijeat.b4962.129219.

[20] M. S. Rizqulloh, F. A. Pamuji, and H. Suryoatmojo, "Design And Simulation Of 10 kW BLDC Motor Speed Control For Electric Vehicles Using FOC Based On Fuzzy Logic Control," *JAREE (Journal on Advanced Research in Electrical Engineering)*, vol. 8, no. 1, 2024, doi: 10.12962/jaree.v8i1.386.

[21] R. Kandiban and R. Arulmozhiyal, "Speed control of BLDC motor using adaptive fuzzy PID controller," *Procedia Engineering*, vol. 38, no. 04, pp. 306–313, 2012, doi: 10.1016/j.proeng.2012.06.039.

[22] P. T., S. G. CS, and A. B. S. Y., "Artificial Neural Networks Based Analysis of BLDC Motor Speed Control," *arXiv*, pp. 1–8, 2021, doi: 10.48550/arXiv.2108.12320.

[23] S. Ye and L. Sun, "Design of PID Intelligent Controller Combining Immune Genetic Algorithm," *Journal of Physics: Conference Series*, vol. 1574, no. 1, 2020, doi: 10.1088/1742-6596/1574/1/012010.

[24] L. K. Agrawal, "Speed control of BLDC motor with neural controller," *Indian Journal of Science and Technology*, vol. 14, no. 4, pp. 373–381, 2021, doi: 10.17485/ijst/v14i4.2164.

[25] A. Tajne, P. Rangari, and D. Bankar, "Review of Performance Of Tuned PID Controller For Speed Control Of DC Motor," *Advance in Electronic and Electric Engineering*, vol. 13, no. 10, pp. 28–31, 2022.

[26] D. Copot, M. Ghita, and C. M. Ionescu, "Simple alternatives to PID-type control for processes with variable time-delay," *Processes*, vol. 7, no. 3, pp. 1–16, 2019, doi: 10.3390/pr7030146.

[27] M. Gajić *et al.*, "Behavior Analysis of the New PSO-CGSA Algorithm in Solving the Combined Economic Emission Dispatch Using Non-parametric Tests," *Applied Artificial Intelligence*, vol. 38, no. 1, 2024, doi: 10.1080/08839514.2024.2322335.

[28] G. A. Sultan, A. F. Sheet, S. M. Ibrahim, and Z. K. Farej, "Speed control of DC motor using fractional order PID controller based on particle swarm optimization," *Indonesian Journal of Electrical Engineering and Computer Science*, vol. 22, no. 3, pp. 1345–1353, 2021, doi: 10.11591/ijeecs.v22.i3.pp1345-1353.

[29] I. Anshory, D. Hadidjaja, and I. Sulistiyowati, "Measurement, Modeling, and Optimization Speed Control of BLDC Motor Using Fuzzy-PSO Based Algorithm," *Journal of Electrical Technology UMY*, vol. 5, no. 1, pp. 17–25, 2021, doi: 10.18196/jet.v5i1.12113.

[30] P. Bhandari *et al.*, "Application of Particle Swarm Optimization (PSO) Algorithm for PID Parameter Tuning in Speed Control of

Brushless DC (BLDC) Motor," *Journal of Physics: Conference Series*, vol. 2570, no. 1, 2023, doi: 10.1088/1742-6596/2570/1/012018.
[31] S. M. Y. Younus, U. Kutbay, J. Rahebi, and F. Hardalaç, "Hybrid Gray Wolf Optimization–Proportional Integral Based Speed Controllers for Brush-Less DC Motor," *Energies*, vol. 16, no. 4, 2023, doi: 10.3390/en16041640.
[32] A. RamaKrishnan, A. Shunmugalatha, and K. Premkumar, "An Improved Tuning of PID Controller for PV Battery-Powered Brushless DC Motor Speed Regulation Using Hybrid Horse Herd Particle Swarm Optimization," *International Journal of Photoenergy*, vol. 2023, 2023, doi: 10.1155/2023/2777505.
[33] R. Alizadehsani *et al.*, "Swarm Intelligence in Internet of Medical Things: A Review," *Sensors*, vol. 23, no. 3, pp. 1–25, 2023, doi: 10.3390/s23031466.
[34] D. Marcsa and M. Kuczmann, "Design and control for torque ripple reduction of a 3-phase switched reluctance motor," *Computers and Mathematics with Applications*, vol. 74, no. 1, pp. 89–95, 2017, doi: 10.1016/j.camwa.2017.01.001.
[35] M. H. Weik, "Total Harmonic Distortion," *Computer Science and Communications Dictionary*, pp. 1798–1798, 2000, doi: 10.1007/1-4020-0613-6_19767.

BIOGRAPHIES OF AUTHORS

Fitriaty Pangerang received a Bachelor's degree in Electrical Engineering from Hasanuddin University, Indonesia, in 2002, majoring in telecommunications. Obtained a Master's degree in electronic systems, control and computers from Hasanuddin University, Indonesia in 2009. Currently he is a teaching staff in the electronics engineering study program, electrical engineering major at the State Polytechnic of Ujung Pandang State, Makassar Indonesia and is currently pursuing doctoral studies at in Electrical Engineering, Hasanuddin University, Indonesia, with a dissertation topic on control optimization of BLDC motors. She can be contacted at email: fitriaty_p@poliupg.ac.id.

Faizal Arya Samman is a professor in the Department of Electrical Engineering, at Hasanuddin University, Indonesia. He received bachelor of engineering degree in electrical engineering from Gadjah Mada University, Indonesia, in 1999 and master of engineering degree from Bandung Institute of Technology with a scholarship award from the Indonesian Ministry of National Education, in 2002. He received his Ph.D. degree from Technische Universität Darmstadt, Germany with a scholarship award from Deutscher Akademischer Austausch-Dienst (DAAD, German Academic Exchange Service), in 2010. He worked toward the postdoctoral research in LOEWE-Zentrum adaptronik-research, innovation, application (AdRIA) within the research cooperation framework between Technische Universität Darmstadt and Fraunhofer Institut LBF in Darmstadt, in 2012. His research interests include multiprocessor system-on-chip, computer architecture, analog and digital integrated electronics, power electronics for renewable energy systems and electric vehicles applications, FPGA/CPLD-based digital system design, energy harvesting, and internet of things. He is a member of the IEEE. He can be contacted at email: faizalas@unhas.ac.id.

Zahir Zainuddin holds a Doctor of Computer Engineering from Bandung Institute of Technology, Indonesia, in 2004. He also received his B.Sc. in Department of Electrical Engineering, Hasanuddin University, Indonesia, in 1988 and his M.Sc. (Computer Engineering) from Florida Institute of Technology USA in 1995. He is an associate professor at the Department of Informatics at Hasanuddin University in Indonesia. His research includes Computer Systems, intelligent systems, computer vision, and smart cities. He has published over 60 papers in international journals and conferences. In 1989, he was a JSPS research fellow at the Tokyo Institute of Technology. He can be contacted at email: zahir@unhas.ac.id.

Rhiza S. Sadjad is a retired senior lecturer in the Department of Electrical Engineering, at Hasanuddin University, South Sulawesi, Indonesia. He received his bachelor's degree in Electrical Engineering from the Institute of Technology Bandung, West Java, Indonesia, in 1981. His master's degree from the University of Wisconsin-Madison, USA, in 1989 and also Ph.D. degree in Electrical Engineering from the University of Wisconsin–Madison, USA, in 1994. His research interests are in the field of automatic control and control systems. He can be contacted at email: rhiza@unhas.ac.id.